J Ginseng Res 45 (2021) 98–107

Contents lists available at ScienceDirect

Journal of Ginseng Research

journal homepage: http://www.ginsengres.org

Research Article

Acremonidin E produced by *Penicillium* sp. SNF123, a fungal endophyte of *Panax ginseng*, has antimelanogenic activities

Kyuri Kim [1], Hae-In Jeong [2], Inho Yang [3], Sang-Jip Nam [2,**], Kyung-Min Lim [1,*]

[1] College of Pharmacy, Ewha Womans University, Seoul, Republic of Korea
[2] Department of Chemistry and Nanoscience, Global Top 5 Program, Ewha Womans University, Seoul, Republic of Korea
[3] Department of Convergence Study on the Ocean Science and Technology, Korea Maritime and Ocean University, Busan, Republic of Korea

ARTICLE INFO

Article history:
Received 16 August 2019
Received in Revised form
13 November 2019
Accepted 15 November 2019
Available online 21 November 2019

Keywords:
Acremonidin E
Endophytic fungus
Melanogenesis
Panax ginseng
Penicillium sp. SNF12

ABSTRACT

Background: Ginseng extracts and ginseng-fermented products are widely used as functional cosmetic ingredients for their whitening and antiwrinkle effects. Recently, increasing attention has been given to bioactive metabolites isolated from endophytic fungi. However, little is known about the bioactive metabolites of the fungi associated with *Panax ginseng* Meyer.
Methods: An endophytic fungus, *Penicillium* sp. SNF123 was isolated from the root of *P. ginseng*, from which acremonidin E was purified. Acremonidin E was tested on melanin synthesis in the murine melanoma cell line B16F10, in the human melanoma cell line MNT-1, and in a pigmented 3D-human skin model, Melanoderm.
Results: Acremonidin E reduced melanogenesis in α-melanocyte-stimulating hormone (α-MSH)-stimulated B16F10 cells with minimal cytotoxicity. qRT–PCR analysis demonstrated that acremonidin E downregulated melanogenic genes, including tyrosinase and tyrosinase-related protein 1 (TRP-1), while their enzymatic activities were unaffected. The antimelanogenic effects of acremonidin E were further confirmed in MNT-1 and a pigmented 3D human epidermal skin model, Melanoderm. Immunohistological examination of the Melanoderm further confirmed the regression of both melanin synthesis and melanocyte activation in the treated tissue.
Conclusion: This study demonstrates that acremonidin E, a bioactive metabolite derived from a fungal endophyte of *P. ginseng*, can inhibit melanin synthesis by downregulating tyrosinase, illuminating the potential utility of microorganisms associated with *P. ginseng* for cosmetic ingredients.

1. Introduction

In recent years, with the rapid growth of the cosmetics market, the demand for raw materials for functional cosmetics like skin whiteners, antiwrinkle creams, sunscreens, antihair loss products, acne treatments, and skin moisturizers is increasing. Especially in Korea and China, where white skin without blemish or pigmentation is highly regarded, this demand has led to rapid expansion in the markets for whitening cosmetics and ingredients. In addition, there is a growing interest in cosmetic materials derived from natural substances that are environmentally friendly [6,9]. In this context, there is a push to discover new skin whitening ingredients that can be produced from natural sources.

Tyrosinase is a crucial enzyme in melanin synthesis, and inhibition of tyrosinase catalytic activity has been a fundamental approach in the search for new skin whitening ingredients. Tyrosinase inhibitors that are widely used as skin-whitening agents include hydroquinone (HQ), arbutin, kojic acid, azelaic acid, L-ascorbic acid, ellagic acid, and tranexamic acid, although these compounds may have drawbacks and some toxicity [36,38]. HQ had been the most popular hypopigmenting agent in the market for more than 50 years, but the safety of HQ remains controversial [16,31,35,38]. Many studies report that HQ may cause exogenous ochronosis in humans, and that benzene metabolites of HQ may cause bone marrow toxicity. There have also been reports of hepatic adenomas, renal adenomas, and leukemia associated with HQ use [16,31]. The use of HQ in cosmetics has been banned in Europe

* Corresponding author. College of Pharmacy, Ewha Womans University, Seoul, 03760, Republic of Korea.
** Corresponding author. Department of Chemistry and Nanoscience, Global Top 5 Program, Ewha Womans University, Seoul, 03760, Republic of Korea.
E-mail addresses: sjnam@ewha.ac.kr (S.-J. Nam), kmlim@ewha.ac.kr (K.-M. Lim).

https://doi.org/10.1016/j.jgr.2019.11.007
p1226-8453 e2093-4947/$ – see front matter

(since March 2000), as well as by the Food and Drug Administration in the United States [7]. Arbutin is chemically unstable and shares most of the side effects of HQ since it works as a prodrug of HQ [50]. Kojic acid is also unstable and may be a potential carcinogen [10]. Azelaic acid causes skin irritation, and the long-term application of retinoids may cause erythema, dryness, and scaling [8]. These adverse effects and the instability of existing whitening cosmetic ingredients have led to a search for new active hypopigmenting compounds with improved safety [29].

Panax ginseng is one of the most studied of the known medicinal plants. It has a wide range of bioactivities that have been reported in the literature, such as antiviral [17] and antitumor activity [1], and in the treatment of obesity [32], Alzheimer's disease [21] and cardiovascular disease [22]. Furthermore, ginseng contains numerous active components, including ginsenoside, polysaccharides, peptides, polyacetylenic alcohols, and fatty acids [2]. Research on this useful plant has been extended to related species, such as Indian and Chinese ginseng (*Withania somnifera* and *Panax notoginseng* [11,43]). In addition, research on the microbes that live on *P. ginseng* has revealed a wide range of associated fungal strains, such as *Entrophospora* spp., *Phoma radicina*, *Alternaria arborescens*, and *Fusarium solani* [37,49]. These endophytes show preferential dwelling to certain parts of *P. ginseng* and their distribution changes over the age of the *P. ginseng* plant. Previous studies have shown a beneficial relationship between the fungi and the host, *P. ginseng* [36,40].

The biosynthetic potential of these endophytes is of interest to researchers [34,41,46]. The most famous example is the anticancer agent taxol, derived from an endophytic fungus of the Pacific yew [15,45,48,51]. Interestingly, several cytotoxic macrolides were isolated from an endophyte of *P. notoginseng* in 2017 [44]. However, most of the interest in the endophytic microbial strains of *P. ginseng* has been mainly directed toward industrial applications for increasing ginsenoside yield [40] or for ginseng pathogen control [36].

The skin whitening effects of the crude extracts and fermented products of ginseng have been studied [27,30,39], and the whitening effects of ginseng extract and ginsenosides have been described in detail. Ginsenoside Rh4 aglycone [18], ginsenoside Rb1 [42], and ginsenoside F1 [13] all show potent whitening activity and have been used in ginseng-based functional cosmetic products for skin whitening. We isolated acremonidin E (**1**) from an endophytic fungus *Penicillium citrinum* sp. SNF123 dwelling in the root of *P. ginseng*. Here, we report on the purification of the fungal metabolite acremonidin E (**1**) and its antimelanogenic effects in an effort to illuminate the cosmetic and therapeutic utility of microorganisms associated with *P. ginseng*.

2. Materials and methods

2.1. Instruments and data collection

Isolation of extracts was conducted by binary HPLC pump (WATERS 600, Waters Co., Milford, MA, USA) and UV-vis detector (WATERS 996 PDA, Waters Co.) was conducted using reversed-phase Phenomenex Luna 5 μ C_{18} column (250 × 10.00 mm, 5 μm, Waters Co.) at a flow rate of 2.0 mL/min. Low-resolution LC-MS data were measured using an HPLC (Agilent Technologies, Santa Clara, CA, USA) with a reversed-phase Phenomenex Luna 5μm C_{18} column (4.6 × 100 mm, 5 μm) at a low flow rate of 1.0 mL/min. NMR spectra were recorded on 300 and 125 MHz for ^{1}H and ^{13}C NMR (Bruker Advance, Billerica, MA, USA), respectively, using the solvent DMSO-d_6 (Cambridge Isotope Laboratories, Inc. Tewksbury, MA, USA). EP grade solvents (Dae-Jung Chemicals & Metals Co. Ltd, Seoul, Korea) were used for fractionation of extracts. For HPLC analyses and LC-MS, HPLC grade solvents were used (J.T.Baker and Dae-Jung Chemicals & Metals Co. Ltd.).

2.2. Fungal strain

The fungal strain SNF123 was isolated from the root of *P. ginseng*. Fiber roots from six-year-old ginseng plants were lightly rinsed with sterile water and placed on a potato dextrose agar (PDA) plate. After the fungus colony formation, subcultures were performed to isolate a single fungal strain. It was classified as *Penicillium* sp. according to the internal transcribed spacer analysis by 93.6% similarity with *Penicillium citrinum* (GenBank accession no. JX192960.1).

2.3. Cultivation and extraction

Endophytic fungal strain SNF123 was cultured on a Potato Dextrose Agar (PDA) plate at room temperature for 7 days. The agar plugs (0.5 × 0.5 cm, 10 pieces each) were inoculated into 1 L of Potato Dextrose Broth (PDB) media in nine 2.5-L Ultra Yield Flasks at 25 °C with shaking at 150 RPM. After 7 days, the filtered fungal broth (9 L) was extracted with ethyl acetate (EtOAc) (9 L) at room temperature. Separated mycelia and spore were extracted with acetone-methanol (1:1 v/v) and were sonicated for 30 min. Both the acetone-methanol and the EtOAc soluble layers were evaporated to afford organic extract.

2.4. Purification

The crude extract was fractioned by silica gel vacuum flash chromatography using series mixtures of dichloromethane and methanol as eluents (seven fractions in the gradient, from 0 to 100% methanol in dichloromethane). The 70% dichloromethane-methanol fraction (517.7 mg) was subjected to preparative HPLC (water:acetonitrile = 45:55), 7.0 mL/min to afford compound **1** (60.3 mg).

*Acremonidin E (**1**)*: ^{1}H and ^{13}C NMR data, Table 1; LRMS *m/z* 319.1 $[M + H]^{+}$.

2.5. Cell culture

The B16F10 cell line from C57BL/6 mice (Manassas, VA, USA) was maintained in standard culture conditions. The Dulbecco's Modified Eagle's Medium (DMEM) was supplemented with antibiotics

Table 1
NMR data of acremonidin E (**1**, DMSO-d_6)[a]

No.	δc, mult.[b]	δ_H (*J* in Hz)	COSY	HMBC
1	167.9, qC			
2	112.3, qC			
3	141.2, CH			
4	117.4, CH	6.93, d (*J* = 8.8 Hz)	5	2
5	122.1, CH	6.81, d (*J* = 8.8 Hz)	4	3,7
6	146.5, CH			
7	131.1, qC			
8	199.9, qC			
9	108.9, qC			
10	162.2, CH			12
11	107.4, qC	6.11, s		15
12	147.4, qC			
13	107.4, CH	6.11, s		15
14	162.2, CH			12
15	22.3, CH_3	2.17, s		
16	52.5, OCH_3	3.55, s		1
3-OH		11.37, br s		
6-OH		11.37, br s		
10-OH		9.20, br s		
14-OH		9.70, br s		

[a] 300 MHz for ^{1}H NMR and 125 MHz for ^{13}C NMR.
[b] Multiplicity was determined by analysis of 2D spectra.

(100 U/mL of penicillin A and 100 U/mL of streptomycin) and 10% fetal bovine serum (FBS) at 37 °C in a humidified atmosphere containing 5% CO_2. At 80% cell confluence, adherent cells were detached with a solution of 0.05% trypsin (Hyclone, South Logan, UT, USA). MNT-1 cells were maintained in minimum essential medium supplemented with 10% DMEM, 20% fetal bovine serum (FBS), 1 M HEPES, and streptomycin-penicillin (100 U/mL each) at 37 °C in a humidified atmosphere containing 5% CO_2. Monolayers of 80% confluent cells were cultured with 0.05% trypsin (Hyclone, South Logan, UT, USA).

2.6. Melanin assay and cell viability assay

For measuring the melanin content, B16F10 cells were cultured into 48-well plates. The serum-starved cells were treated with various concentrations of compound **1** in culture medium containing 0.5% dimethyl sulfoxide (DMSO) and 200 nM α-MSH for 48 h. α-MSH was used to induce melanin synthesis in all experiments, as described previously [23]. α-MSH-untreated cells were used as negative controls, and arbutin-treated cells were used as positive controls. After cells were dissolved in 200 μL of 1 *N* NaOH at 60 °C for 1 h in the dark, the total melanin content was measured by absorbance at 405 nm using a microplate reader (Spectra max 190, Molecular Devices, Sunnyvale, CA, USA) as the previous study [24]. 3-(4,5-dimethylthiazol-2-yl)-2,5-diphenyltetrazolium bromide (MTT) was used to measure cell viability. B16F10 cells were incubated with 0.25 mL of 0.5 mg/mL MTT solution in DMEM for 2 h at 37 °C. Blue formazan dye was dissolved in 0.25 mL of DMSO for 30 min, and 200 μL of supernatant was measured by the absorption value at 540 nm. All measurements were performed in triplicate.

2.7. Mushroom tyrosinase inhibition assay

In vitro cell-free system assay was performed to determine whether compound **1** showed any direct inhibitory effect against tyrosinase, a key enzyme in melanogenesis. 180 μL of 0.03% tyrosine in 0.1 M potassium phosphate was added to 20 μL of mushroom tyrosinase (250 units), and 180 μL of 0.2% L-DOPA in 0.1 M potassium phosphate was mixed with 50 units of mushroom tyrosinase. 2 μL of DMSO (final 0.5%) containing compound was added and incubated at 37 °C for the indicated time. The absorbance was measured at 475 nm (Spectra max 190, Molecular Devices, Sunnyvale, CA, USA).

2.8. RNA isolation and real-time PCR

B16F10 cells were washed twice with phosphate-buffered saline after a 24 h exposure with compound **1** and were lysed using Trizol (Invitrogen, CA, USA). After the addition of chloroform, samples were centrifuged at 12,000 rpm for 10 min. The aqueous phase was mixed with isopropanol, and RNA pellets were collected by centrifugation (12,000 rpm, 15 min, 4 °C). RNA pellets were washed with 70% ethanol and dissolved in RNase-free, diethylpyrocarbonate (DEPC)-treated water (Waltham, MA, USA). The RNA yield was estimated by determining the optical density at 260 nm with a spectrophotometer (NanoDrop Technologies, INC., Wilmington, DE, USA). Relative expression levels of mRNA were measured by quantitative real-time PCR. cDNA was synthesized from 1,250 ng of total RNA with oligo(dT) (Bioelpis, Seoul, Korea). A SYBR Green PCR master mix and a StepOnePlusTM Real-time PCR machine (Applied Biosystems, Warrington, UK) were used in each reaction. The sequence of primers was as follows: forward tyrosinase, 5′-G GGCCC AAATTGTACAGAGA-3′; reverse tyrosinase, 5′-ATGGGTGTT-GACCATTGTT-3′; forward TRP-1, 5′-GTTCAATGGCCAGGTCAGGA-3′; and reverse TRP-1, 5′-CAGACAAGAAGCAACCCCGA-3′. Cycling parameters were 50 °C for 2 min, 95 °C for 10 min, 40 cycles of 95 °C for 15 s, and 50 °C for 1 min.

2.9. Western blot analysis

After 24 or 48 h of exposure to compound **1**, B16F10 cells were homogenized in RIPA buffer (Sigma, MO, USA) containing a 1% protease inhibitor cocktail and 1 mM phenylmethanesulfonyl fluoride (PMSF) (Sigma, MO, USA). The supernatant of the homogenate was collected, and the protein concentration was determined by BCA assay. Equal amounts of protein were subjected to 10% sodium dodecyl sulfate-polyacrylamide gel electrophoresis (SDS-PAGE) and transferred to nitrocellulose membranes (Amersham, Buckinghamshire, UK). After being blocked at room temperature in 5% BSA for 1 h, the blots were probed with each of the following primary antibodies against each target protein in 1 × TBST for 2 h at room temperature: mouse antityrosinase monoclonal antibody (1:2000 dilution: Abfrontier, Seoul, Korea). HRP-conjugated secondary antibodies (KPL, Gaithersburg, MD, USA) were used to detect bound antibodies, and the immune reactive bands were visualized using ECL western blotting detection reagents (Amersham Biosciences, Little Chalfont, UK) and by Amersham Imager 600 (GE healthcare life sciences, UK). β-actin antibody (Santa Cruz Biotechnology, Santa Cruz, CA, USA) was used as a control for immunoblotting.

2.10. Antipigmenting assay with a pigmented human epidermal 3D skin model

Melanoderm™ (MatTek, MA, USA) is an artificial human epidermis consisting of normal human epidermal keratinocytes and normal human melanocytes (NHM) that exhibit uniform and highly reproducible morphological and ultrastructural characteristics. Tissues containing NHM from donors of color become increasingly pigmented maintaining a normal epithelial morphology. Melanoderm was pre-incubated for 24 h, then treated with the indicated compounds every other day for 14 days.

For the histological examination, all samples were fixed in 4% phosphate-buffered formalin (PFA) for 24 h with gentle shaking. Fixed samples were paraffin-embedded and cut into 5-μm sections using microtome (RM2335, Leica, Wetzlar, DE). Hematoxylin and eosin staining (H&E) was performed one day after sectioning. For H&E staining, paraffin sections were deparaffinized and then

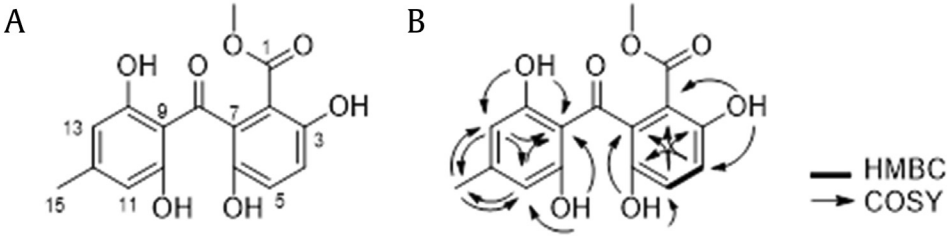

Fig. 1. (A) Chemical structure and (B) COSY and key KMBC correlations of acremonidin E (**1**).

hydrated in descending ethanol concentrations. Next, sections were stained with 0.1% Mayer's hematoxylin for 10 min and 0.5% eosin in 95% EtOH. After staining with H&E, the washing steps were immediately and sequentially performed as follows: dipped in distilled H_2O until eosin stops streaking, dipped in 50% EtOH 10 times, dipped in 70% EtOH 10 times, incubated in 95% EtOH for 30 s, and incubated in 100% EtOH for 1 min. Then, samples were covered with the mounting solution (6769007, Thermo Scientific, MA, USA) and examined under the light microscope (BX43, OLYMPUS, Shinjuku, JP).

For Melan A staining, paraffin-embedded samples were cut into 5-μm sections. Sections were deparaffinized and rehydrated as described above. After rehydration steps, unmasking was performed using pH 6.0 antigen retrieval solution (S1699, DAKO, Carpinteria, CA, USA) with high pressure, followed by ice bucket cooling until the solution looked transparent. Next, sections were incubated in 3% H_2O_2 for 30 min to block endogenous peroxidase and washed two times with PBS. The blocking step to reduce nonspecific signal was conducted by incubating the samples with ample drops of Protein Block Serum-Free (X0909, DAKO, Carpinteria, CA, USA) for 1–2 h at room temperature. AntiMelan A antibody (1:1000, M719629, DAKO, Carpinteria, CA, USA) were diluted in antibody diluent (S2022, DAKO, Carpinteria, CA, USA) and incubated overnight at 4 °C in a humidity chamber. After three washes in PBS, sections were incubated with HRP-conjugated antimouse secondary antibody (K4001, DAKO, Carpinteria, CA, USA) for 15 min at room temperature. For immunohistochemistry, DAB (K3468, DAKO, Carpinteria, CA, USA) was used for the development of HRP-conjugated antibodies, and Mayer's hematoxylin (S3309, DAKO, Carpinteria, CA, USA) was used for counterstaining.

For Fontana-Masson's argentaffin staining, paraffin sections were incubated with ammoniacal silver nitrate for 1 h at 60 °C, followed by two washes with distilled water. For color development, samples were incubated with 0.2% working solution of gold chloride for 10 min and immediately rinsed 10 times with distilled water. After the final washes, samples were incubated with 5% sodium thiosulfate for 5 min to fix silver and rinsed with running water for 1 min. After silver fixation, nuclear fast red (60700, Fluka, Ronkonkoma, NY, USA) was used for counterstaining, and samples were rinsed with running water for 1 min.

2.11. Statistics

Data are expressed as mean ± SEM of three or more independent experiments. The statistical significance of differences between groups was assessed using a two-sided Student's *t*-test. A *p*value < 0.05 was considered significant.

3. Results

3.1. Isolation of compound 1 from endophytic fungi in P. ginseng

Compound **1** was isolated as a brown amorphous powder, and its molecular formula was determined to be $C_{16}H_{14}O_7$ based on the analysis of LRMS data (a pseudomolecular ion peak at *m/z* 319.1) and interpretation of ^{13}C NMR data. The presence of a conjugated aromatic or phenolic moiety was inferred from strong UV absorptions at 207, 281, and 342 nm. The ^1H NMR spectrum showed four phenolic protons (δ_H 11.37, 11.37, 9.70, 9.20), four aromatic protons (δ_H 6.93, 6.81, 6.11, 6.11), and two methyl singlets (δ_H 3.55, 2.17). The ^{13}C NMR and HSQC spectroscopic data revealed two carbonyls, eight quaternary carbons, and two methyl carbons. A phenyl group was detected from HMBC correlations of H-4 to C-2, C-6, and H-5 to C-7, C-3, with correlations of two phenols 3-OH to C-2, C-4, and 6-OH to C-5, C-7. Another phenyl group was identified based on HMBC correlations from H-11 to C-10, C-12, and H-13 to C-12, C-14, with correlations from two phenols 10-OH to C-9, C-11, and 14-OH to C-9, C-13. A methyl group was attached at C-12 by HMBC correlation from CH_3-15 to C-11, C-13. Because all of the aromatic positions of the second phenyl ring were filled except for C-9, the connection of the two phenyl rings was determined to be through a ketone group. The positions of the connecting ketone carbon and the remaining carbonyl carbon on the first ring were determined by the chemical shift of C-6 and C-7, which completed the gross structure of **1** (Fig. 1). Compound **1** was identified as acremonidin E, which was first found in an *Acremonium* sp. to have antibiotic activity [14].

3.2. Acremonidin E (1) inhibits melanogenesis and activation of B16F10 melanoma cells and MNT-1 cells

For investigating the antipigmentary effect of acremonidin E (**1**), α-MSH-stimulated murine melanoma cells, B16F10, were treated with **1** for 48 h. As shown in Fig. 2A, the intracellular melanin content of the cells decreased significantly after treatment with **1** at a concentration range of 2.5–50 μg/mL. Moreover, **1** was not cytotoxic to B16F10 cells up to 50 μg/mL (Fig. 2B).

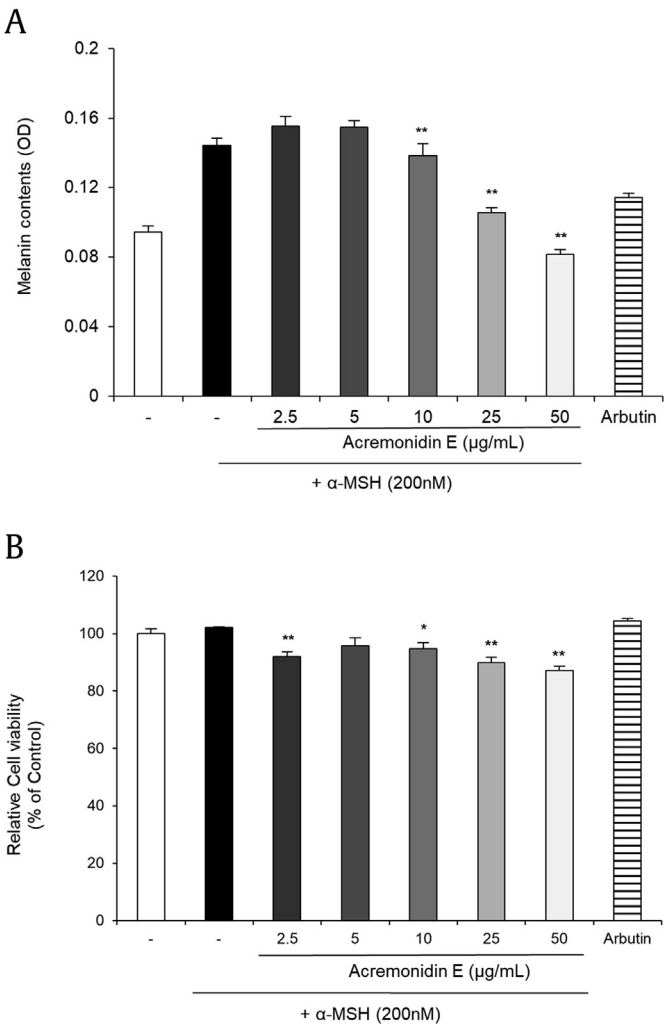

Fig. 2. Effects of acremonidin E (**1**) on melanin content and viability of B16F10 cells. (A) Measured melanin content; (B) Cell viability was determined by MTT assay. The cells were treated with arbutin at 50 μg/mL and with **1** at the indicated concentrations for 48 h. Data are presented as the mean ± standard deviation (SD) ($n = 4$).

The antimelanogenic effects of acremonidin E (**1**) were tested in a pigmented human melanoma cell line, MNT-1. The pellet color of MNT-1 was found to lighten, depending on the concentration of **1** (Fig. 3A). Inhibition of melanocyte activation was demonstrated by the regression of α-MSH-stimulated melanoma cell dendrites after treatment with **1** (Fig. 3B). Dendrite formation in melanocytes is required for melanosome transfer to keratinocytes [26]. For examining the effect of **1** on melanosome transfer from melanocytes to keratinocytes, a coculture system of MNT-1 cells and a human keratinocyte cell line, HaCaT, was used. As shown in Fig. 3C,

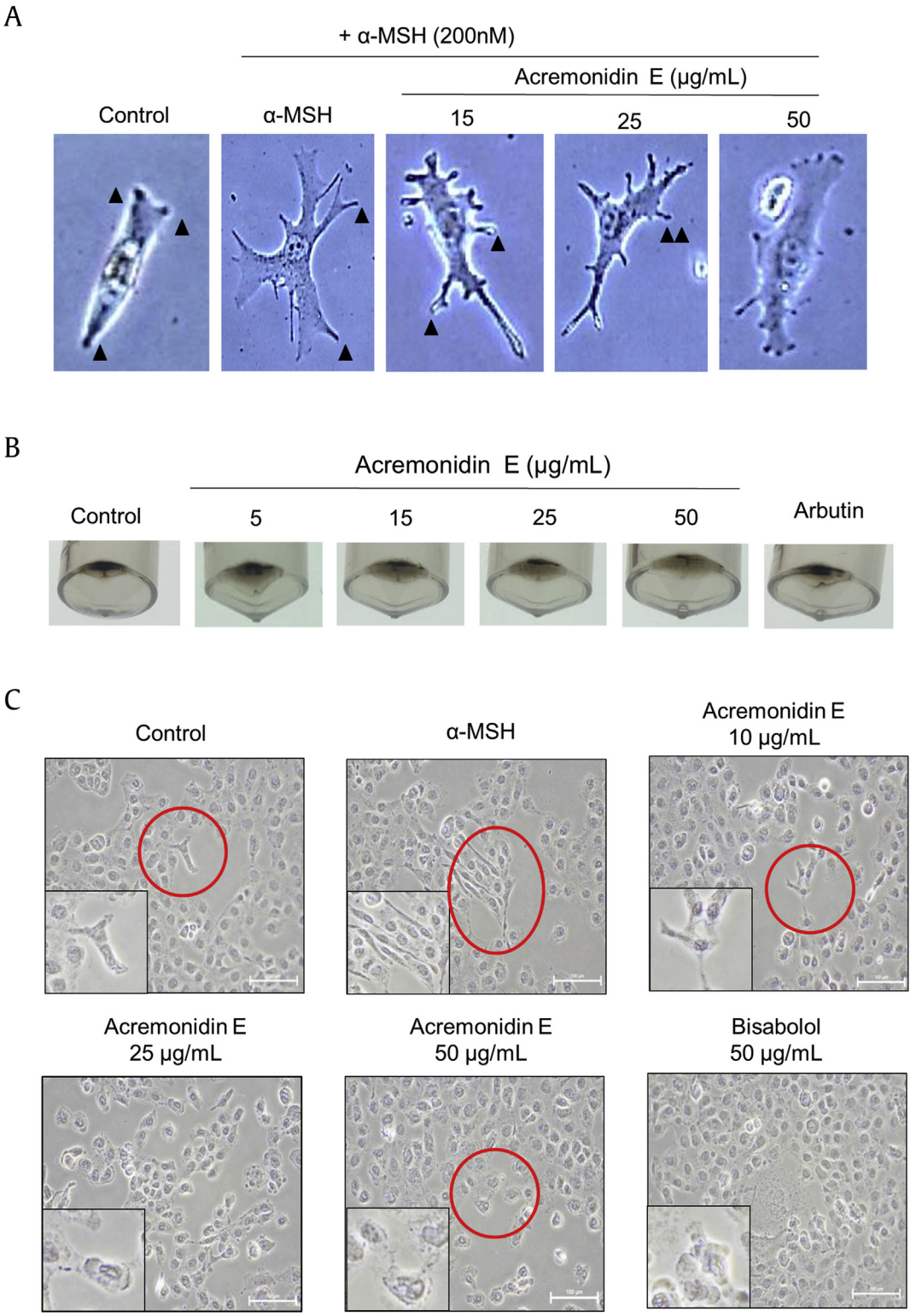

Fig. 3. Effects of acremonidin E (**1**) on dendrite formation in various cell lines. (A) Morphological changes of B16F10 cells; (B) Macroscopic view of MNT-1 cell pellets; (C) Dendrite formation changes in MNT-1/HaCaT coculture cells. The cells were treated with **1** for 24 h, and morphological changes were observed under optical microscopy (400 X). The MNT-1 cell pellets were lysed by RIPA buffer.

the extension of dendrites from MNT-1 cells decreased as the concentration of **1** increased.

3.3. Acremonidin E (1) downregulates the expression of tyrosinase and TRP-1 without affecting enzymatic activity

A cell-free mushroom tyrosinase assay was used to examine whether acremonidin E (**1**) can affect tyrosinase activity [26]. The results showed that **1** did not affect the enzymatic activity of tyrosinase, while arbutin significantly inhibited enzymatic activity. (Fig. 4A and B)

For investigating the expression of melanogenic enzymes, qRT-PCR assay was performed. Acremonidin E (**1**) inhibited tyrosinase, and tyrosinase-related protein 1 (TRP-1) expression in α-MSH stimulated murine melanoma cells (B16F10). (Fig. 5A and B). Downregulation of tyrosinase and TRP-1 was further confirmed by

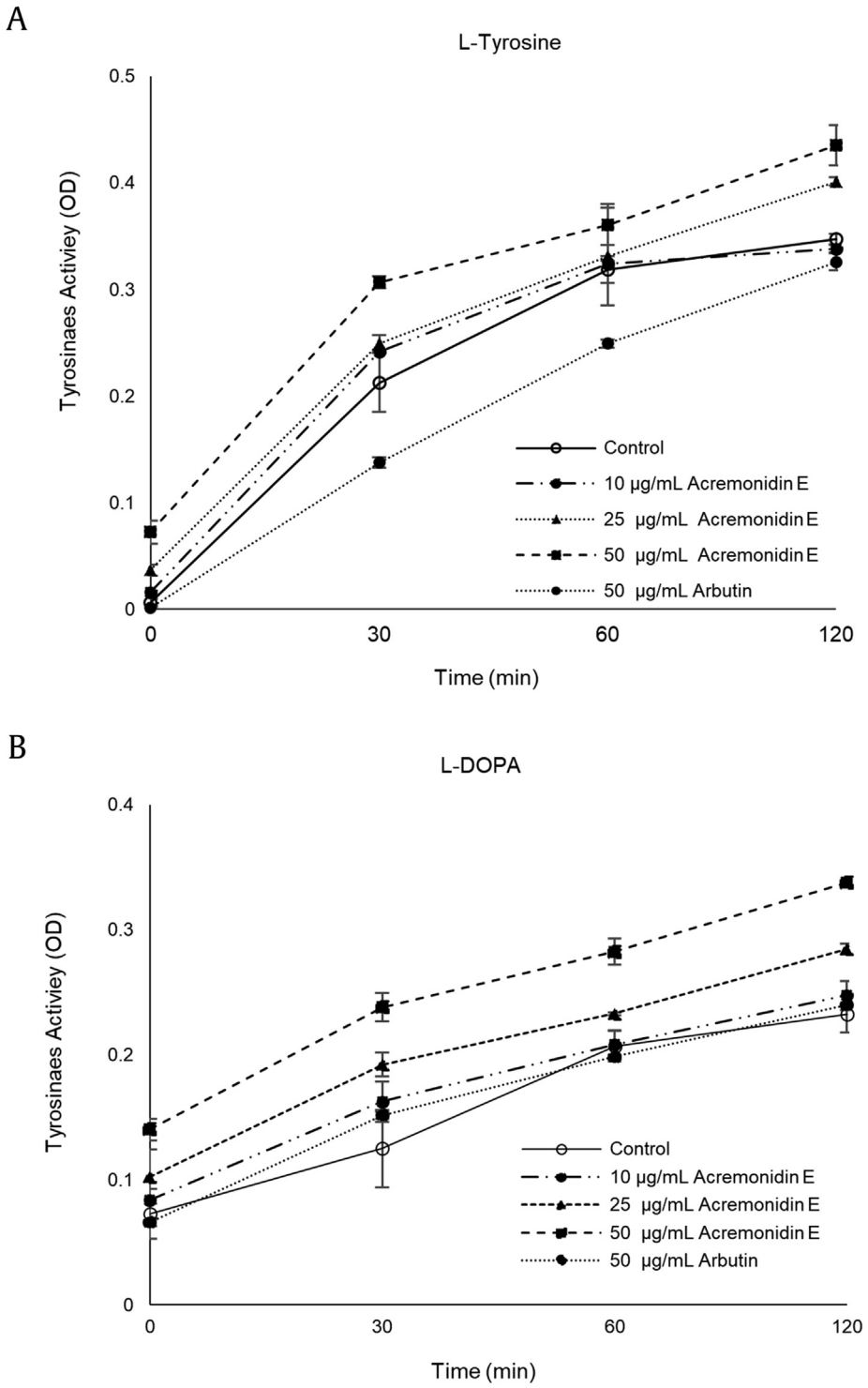

Fig. 4. Effects of acremonidin E (**1**) on mushroom tyrosinase activity. Tyrosinase enzymatic activity was investigated using a mushroom tyrosinase assay with (A) L-tyrosine and (B) L-DOPA (3,4-dihydroxyphenylalanine) as substrates. Data are presented as the ±SD ($n = 3$).

the immunoblot assay, in which a 48 h application of **1** suppressed protein levels of tyrosinase (Fig. 6A and B) and TRP-1 (Fig. 6C and D).

3.4. Effects of acremonidin E (1) on the Melanoderm™ 3D skin model

The antipigmentary effect of acremonidin E (**1**) was further confirmed using an artificial pigmented human epidermis, Melanoderm (MatTek, Ashland, MA, USA), which is widely used as an alternative to animal testing for melanogenesis-related studies. The color of the skin tissue was significantly lightened after treatment with **1** when compared to untreated skin (Fig. 7A). The skin tissue was fixed, tissue-processed, and stained with H&E, Fontana-Masson (FM) [25,33], and antiMelan A [4] on the last day of the experiment. As shown in Fig. 7B, regression of melanocyte activation and melanogenesis was found after treatment with **1** as determined by decreased melanin content and distribution (Fig. 7B). In addition, the skin irritation test was conducted using Keraskin (Biosolution Co, Seoul, Korea), a reconstructed human epidermis model [20]. Even at high concentrations (0.5%), **1** showed an insignificant level of cytotoxicity when compared to the negative control (Fig. 7C).

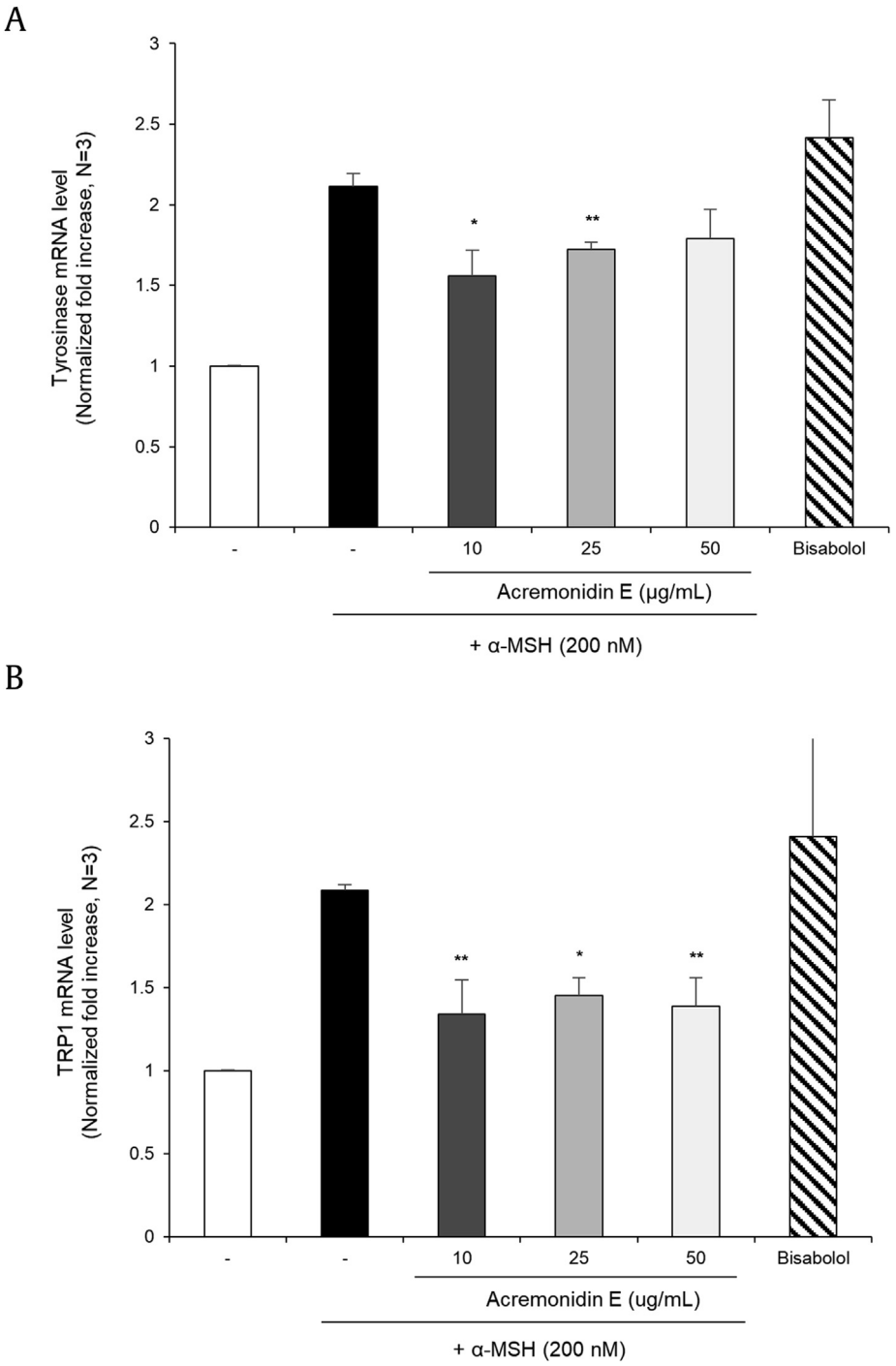

Fig. 5. Effects of acremonidin E (**1**) on the mRNA level of B16F10 cells. mRNA expression levels of (A) tyrosinase; (B) TRP-1 in B16F10 cells were determined by real-time PCR. The cells were treated with **1** and bisabolol at the indicated concentrations for 24 h. Data are presented as the mean ± SD ($n = 3$, $^{*}p < 0.05$ and $^{**}p < 0.01$).

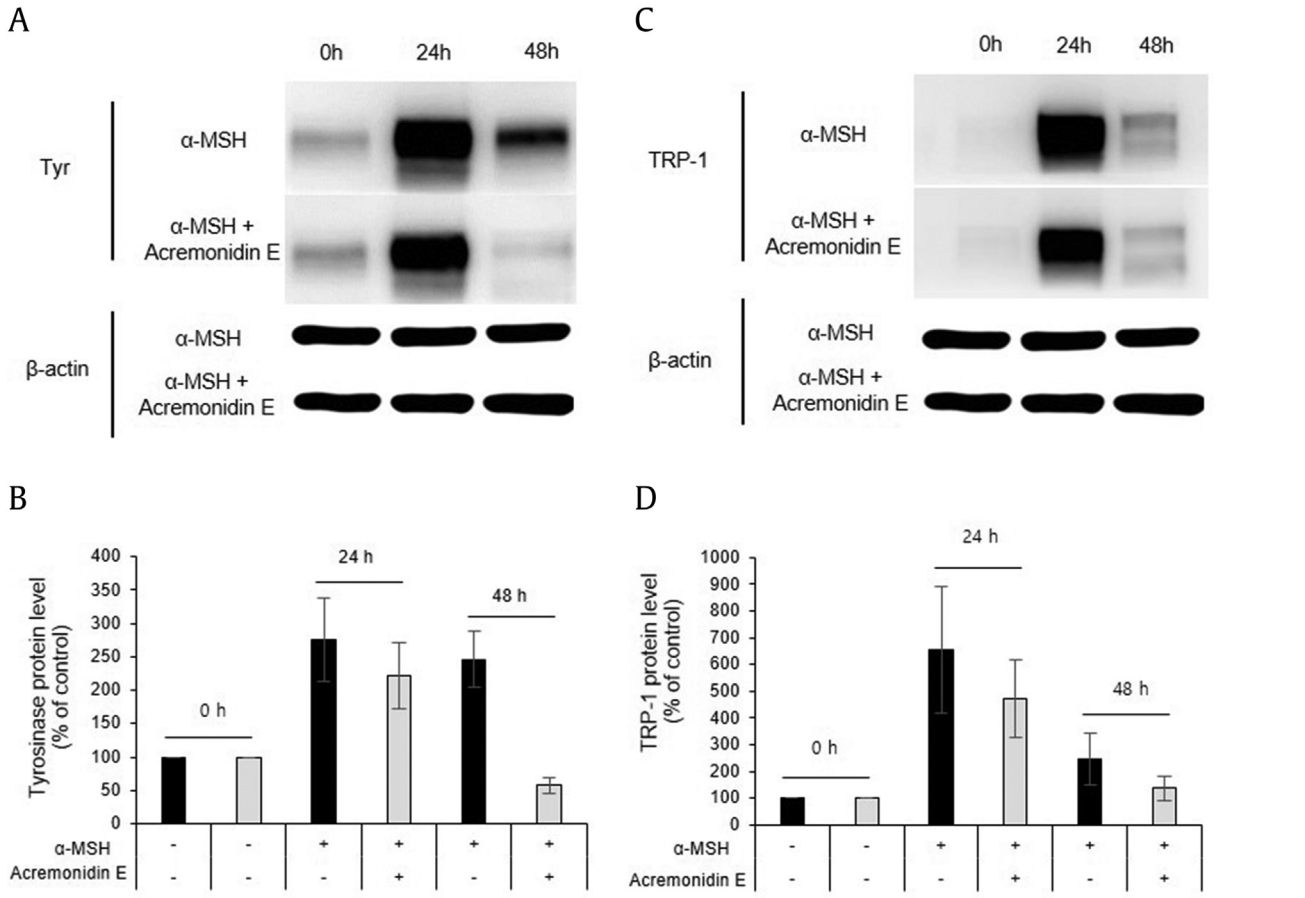

Fig. 6. Effects of acremonidin E (**1**) on protein levels in B16F10 cells. Tyrosinase and TRP-1 protein levels were determined by western blotting. (A) Tyrosinase protein levels; (B) Quantitation of tyrosinase protein level; (C) TRP-1 protein levels; (D) Quantitation of TRP-1 protein level. The cells were treated with **1** at a concentration of 25μL for the indicated times. The quantitation of the western blot band was analyzed by Multi Gauge V3.0 software.

4. Discussion

In this study, we isolated acremonidin E (**1**) from an endophytic fungus, *Penicillium* sp., found on the root of *P. ginseng*. We also demonstrated that **1** suppressed α-MSH-stimulated melanin in a murine melanoma cell line, B16F10, with minimal cytotoxicity. Compound **1** also suppressed the α-MSH-stimulated extension of melanoma cell dendrites. Antimelanogenic activities of **1** were further confirmed in a human melanoma cell line, MNT-1. Notably, compound **1** could suppress α-MSH-stimulated dendrite extension in a coculture of MNT-1 with HaCaT cells (a human keratinocyte cell line). The mRNA expression levels of tyrosinase and TRP-1 were downregulated, which is consistent with other the anti-melanogenic effects of **1**. Likewise, the protein levels of tyrosinase and TRP-1 were significantly attenuated by the application of **1**.

Antimelanogenic effects of ginsenoside and processed *P. ginseng* extracts have been previously reported [33–35]. Ginsenoside F1, which is a metabolite produced by the hydrolysis of ginsenoside Re and Rg1 in *P. ginseng*, was found to inhibit melanosome transfer in the human epidermis [26]. Inhibitory activity of ginsenoside RH4 aglycon against melanin synthesis in B16 melanoma cells has been studied [36]. The inhibition effect of ginsenoside RB1 against tyrosinase activity has been shown to decrease melanin content in B16 melanoma cells [36]. Also, an ethanol extract of *P. ginseng* berry calyx, Pg-C-EE, has been found to have antimelanogenesis properties by inhibiting melanin synthesis, as well as tyrosinase enzymatic activities [28]. In this study, we demonstrated that acremonidin E (**1**), a secondary metabolite of endophytic fungi, has antipigmentary effects, which could expand the search for other active ingredients in microorganisms associated with *P. ginseng*.

We, for the first time, isolated and purified acremonidin E (**1**) from the endophytic fungus *Penicillium* sp. found in the root of *P. ginseng*. Compound **1** was previously isolated from the endophytic fungus *Acemonium* sp., and found to exhibit antibacterial activity against Gram-positive bacteria. Acremonidins A and B, structurally related to **1**, have also been found to have antibacterial activity against both methicillin-resistant *S. aureus* and vancomycin-resistant *Enterococci* [14]. However, there has been no report on the whitening effects of **1**.

Normally murine melanoma cells are grown in 2D monolayers and are used to investigate the antimelanogenic effects of various substances. However, there are known limitations of 2D monolayers, such as loss of important cell-to-cell signals, key regulators, and tissue phenotypes [3,5,12]. Also, animal cells may show different results than human cells. 3D cell culture mimics the basic structure of human skin and provides a versatile and relevant system for testing new compounds [5]. The 3D-human skin tissue model is used for evaluating the skin-whitening compounds as an alternative to animal testing [19,47]. In this study, we used Melanoderm to investigate the antipigmentary effects of acremonidin E (**1**) and found that the color of the skin tissue was significantly brightened after 14 days of **1** application when compared to untreated skin. Consistently, the stained tissues revealed increased melanin reduction with higher concentrations of **1**. Interestingly, nuclei vacuole and skin tissue

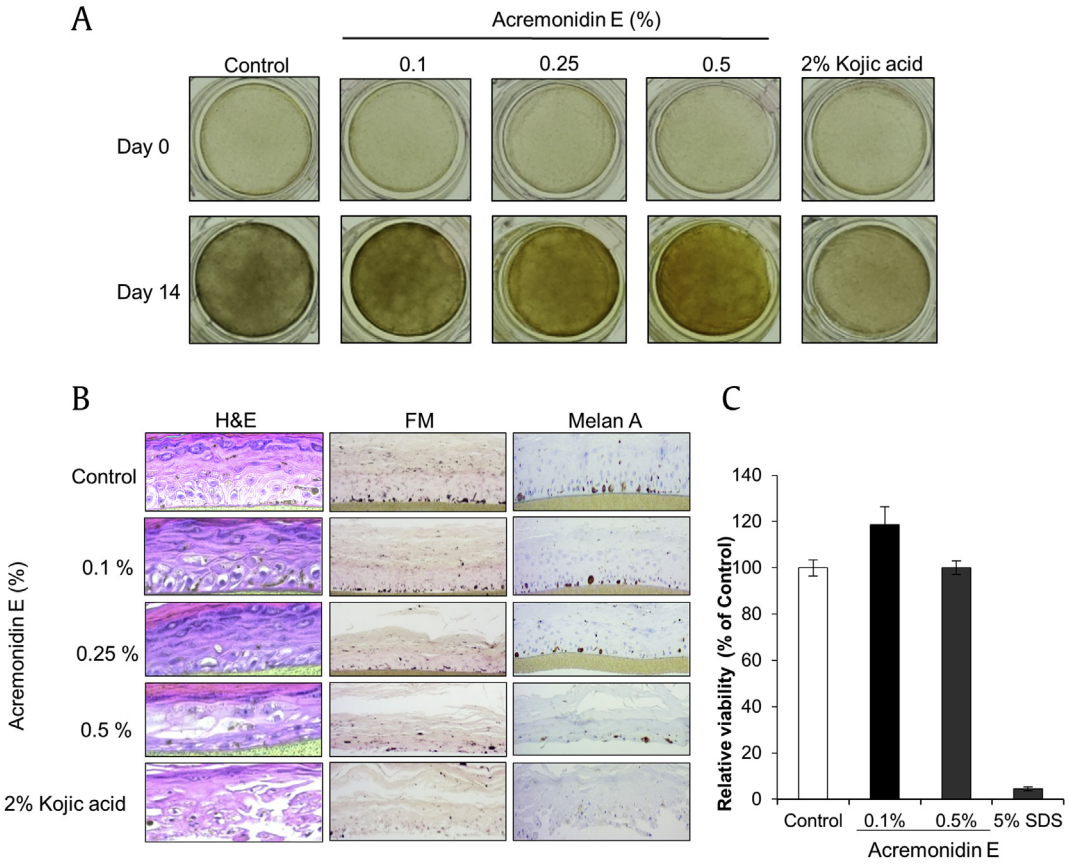

Fig. 7. Effects of acremonidin E (**1**) on the Melanoderm™ 3D skin model. (A) Color of 3D human skin tissue model (Melanoderm; MatTek); (B) hematoxylin and eosin (H & E) stained tissues, Fontana-Masson (FM) stained tissues, and MelanA stained tissues; (C) Cell viability was further confirmed in a 3D reconstituted human epidermis model, Keraskin, using MTT assay. Data are presented as the mean ± SD ($n = 3$).

corrosion appeared after the application of kojic acid, which suggests a cytotoxicity effect from kojic acid while **1** did not show signs of cytotoxicity.

In summary, we isolated acremonidin E (**1**) from an endophytic fungus *Penicillium* sp. found in the root of *P. ginseng* for the first time. We also demonstrated that **1** has antipigmentary effects in both murine and human melanoma cells, and when applied to a 3D pigmented skin model, Melanoderm. Compound **1** downregulated the expression of melanogenic enzymes without affecting enzymatic activity levels or cell viability. We believe that our study will shed light on the utility of the endophytic microorganisms associated with *P. ginseng* as bioactive substances.

Conflicts of interest

All authors have no conflicts of interest to declare.

Acknowledgments

This work was supported by the grants from National Research Foundation (NRF) No. 2018R1D1A1B07042919, and 2018R1A5A2025286.

References

[1] Ahuja A, Kim JH, Kim J-H, Yi Y-S, Cho JY. Functional role of ginseng-derived compounds in cancer. J Ginseng Res 2018;42(3):248–54.
[2] Attele AS, Wu JA, Yuan C-S. Ginseng pharmacology: multiple constituents and multiple actions. Biochem Pharmacol 1999;58(11):1685–93.
[3] Birgersdotter A, Sandberg R, Ernberg I. Gene expression perturbation in vitro—a growing case for three-dimensional (3D) culture systems. In: Seminars in cancer biology, vol. 5. Elsevier; 2005. p. 405–12.
[4] Blessing K, Sanders D, Grant J. Comparison of immunohistochemical staining of the novel antibody melan-A with S100 protein and HMB-45 in malignant melanoma and melanoma variants. Histopathology 1998;32(2):139–46.
[5] Brohem CA, da Silva Cardeal LB, Tiago M, Soengas MS, de Moraes Barros SB, Maria-Engler SS. Artificial skin in perspective: concepts and applications. Pigment Cell & Melanoma Res 2011;24(1):35–50 (1):35–50.
[6] Burger P, Landreau A, Azoulay S, Michel T, Fernandez X. Skin whitening cosmetics: feedback and challenges in the development of natural skin lighteners. Cosmetics 2016;3(4):36.
[7] Chatatikun M, Yamauchi T, Yamasaki K, Aiba S, Chiabchalard A. Anti melanogenic effect of Croton roxburghii and Croton sublyratus leaves in α-MSH stimulated B16F10 cells. J Tradit Complement Med 2019;9(1):66–72.
[8] Draelos Z. Skin lightning preparations and the hydroquinone controversy. Dermatol Ther 2007;20(5):308–13.
[9] Dureja H, Kaushik D, Gupta M, Kumar V, Lather V. Cosmeceuticals: an emerging concept. J Pharmacol 2005;37(3):155.
[10] Fujimoto N, Onodera H, Mitsumori K, Tamura T, Maruyama S, Ito A. Changes in thyroid function during development of thyroid hyperplasia induced by kojic acid in F344 rats. Carcinogenesis 1999;20(8):1567–72.
[11] Ganguly B, Kumar N, Ahmad AH, Rastogi SK. Influence of phytochemical composition on in vitro antioxidant and reducing activities of Indian ginseng [*Withania somnifera* (L.) Dunal] root extracts. J Ginseng Res 2018;42(4):463–9.
[12] Griffith LG, Naughton G. Tissue engineering–current challenges and expanding opportunities. Science 2002;295(5557):1009–14.
[13] Han J, Lee E, Kim E, Yeom MH, Kwon O, Yoon TH, Lee TR, Kim K. Role of epidermal γδ T-cell-derived interleukin 13 in the skin-whitening effect of Ginsenoside F1. Exp Dermatol 2014;23(11):860–2.
[14] He H, Bigelis R, Solum EH, Greenstein M, Carter GT. Acremonidins, new polyketide-derived antibiotics produced by Acremonium sp., LL-Cyan 416. J Antibio 2003;56(11):923–30.
[15] Heinig U, Scholz S, Jennewein SJFd. Getting to the bottom of taxol biosynthesis by fungi. Fungal Divers 2013;60(1):161–70.
[16] Hu Z-M, Zhou Q, Lei T-C, Ding S-F, Xu S-Z. Effects of hydroquinone and its glucoside derivatives on melanogenesis and antioxidation: biosafety as skin whitening agents. J Dermatol Sci 2009;55(3):179–84.

[17] Im K, Kim J, Min H. Ginseng, the natural effectual antiviral: protective effects of Korean Red Ginseng against viral infection. J Ginseng Res 2016;40(4):309–14.
[18] Jeong Y-M, Oh WK, Tran TL, Kim W-K, Sung SH, Bae K, Lee S, Sung J-H. Aglycone of Rh4 inhibits melanin synthesis in B16 melanoma cells: possible involvement of the protein kinase A pathway. Biosci Biotechnol Biochem 2013:120602.
[19] Jones K, Hughes J, Hong M, Jia Q, Orndorff S. Modulation of melanogenesis by aloesin: a competitive inhibitor of tyrosinase. Pigment Cell Res 2002;15(5):335–40.
[20] Jung K-M, Lee S-H, Jang W-H, Jung H-S, Heo Y, Park Y-H, Bae S, Lim K-M, Seok SH. KeraSkin™-VM: a novel reconstructed human epidermis model for skin irritation tests. Toxicol in Vitro 2014;28(5):742–50.
[21] Kim H-J, Jung S-W, Kim S-Y, Cho I-H, Kim H-C, Rhim H, Kim M, Nah S-Y. Panax ginseng as an adjuvant treatment for Alzheimer's disease. J Ginseng Res 2018;42(4):401–11.
[22] Kim J-H. Pharmacological and medical applications of Panax ginseng and ginsenosides: a review for use in cardiovascular diseases. J Ginseng Res 2018;42(3):264–9.
[23] Kim M, Lee C-S, Lim K-M. Rhododenol activates melanocytes and induces morphological alteration at sub-cytotoxic levels. Int J Mol Sci 2019;20(22):5665.
[24] Kim SE, Lee CM, Kim YC. Anti-melanogenic effect of oenothera laciniata methanol extract in melan-a cells. Toxicol Res 2017;33(1):55–62. https://doi.org/10.5487/TR.2017.33.1.055.
[25] Kim Y-M, Cho S-E, Seo Y-K. The activation of melanogenesis by p-CREB and MITF signaling with extremely low-frequency electromagnetic fields on B16F10 melanoma. Life Sci 2016;162:25–32.
[26] Lee C-S, Nam G, Bae I-H, Park J. Whitening efficacy of ginsenoside F1 through inhibition of melanin transfer in cocultured human melanocytes–keratinocytes and three-dimensional human skin equivalent. J Ginseng Res 2019;43(2):300.
[27] Lee H-S, Kim M-R, Park Y, Park HJ, Chang UJ, Kim SY, Suh HJ. Fermenting red ginseng enhances its safety and efficacy as a novel skin care anti-aging ingredient: in vitro and animal study. J Med Food 2012;15(11):1015–23.
[28] Lee J-O, Kim E, Kim JH, Hong YH, Kim HG, Jeong D, Kim J, Kim SH, Park C, Seo DB. Antimelanogenesis and skin-protective activities of Panax ginseng calyx ethanol extract. J Ginseng Res 2018;42(3):389–99.
[29] Lee Y-S, Kim H-K, Lee K-J, Jeon H-W, Cui S, Lee Y-M, Moon B-J, Kim Y-H, Lee Y-S. Inhibitory effect of glyceollin isolated from soybean against melanogenesis in B16 melanoma cells. BMB Rep 2010;43(7):461–7.
[30] Lee Y, Kim K-T, Kim SS, Hur J, Ha SK, Cho C-W, Choi SY. Inhibitory effects of ginseng seed on melanin biosynthesis. Pharmacogn Mag 2014;10(Suppl 2):S272.
[31] Levitt J. The safety of hydroquinone: a dermatologist's response to the 2006 Federal Register. J Am Acad Dermatol 2007;57(5):854–72.
[32] Li Z, Ji GE. Ginseng and obesity. J Ginseng Res 2018;42(1):1–8.
[33] McMullen R, Bauza E, Gondran C, Oberto G, Domloge N, Farra CD, Moore DJ. Image analysis to quantify histological and immunofluorescent staining of ex vivo skin and skin cell cultures. Int J Cosmet Sci 2010;32(2):143–54.
[34] Nisa H, Kamili AN, Nawchoo IA, Shafi S, Shameem N, SA Bandh. Fungal endophytes as prolific source of phytochemicals and other bioactive natural products: a review. Microb Pathog 2015;82:50–9.
[35] Nordlund J, Grimes P, Ortonne JP. The safety of hydroquinone. J Eur Acad Dermatol Venereol 2006;20(7):781–7.
[36] Park Y-H, Kim Y, Mishra RC, Bae H. Fungal endophytes inhabiting mountain-cultivated ginseng (Panax ginseng Meyer): diversity and biocontrol activity against ginseng pathogens. Sci Rep 2017;7(1):16221.
[37] Park Y-H, Lee S-G, Ahn DJ, Kwon TR, Park SU, Lim H-S, Bae H. Diversity of fungal endophytes in various tissues of Panax ginseng Meyer cultivated in Korea. J Ginseng Res 2012;36(2):211.
[38] Pillaiyar T, Manickam M, Namasivayam V. Skin whitening agents: medicinal chemistry perspective of tyrosinase inhibitors. J Enzyme Inhib Med Chem 2017;32(1):403–25.
[39] Song M, Mun J-H, Ko H-C, Kim B-S, Kim M-B. Korean Red Ginseng powder in the treatment of melasma: an uncontrolled observational study. J Ginseng Res 2011;35(2):170.
[40] Song X, Wu H, Yin Z, Lian M, Yin C. Endophytic bacteria isolated from Panax ginseng improves ginsenoside accumulation in adventitious ginseng root culture. Molecules 2017;22(6):837.
[41] Uzma F, Mohan CD, Hashem A, Konappa NM, Rangappa S, Kamath PV, Singh BP, Mudili V, Gupta VK, Siddaiah CN. Endophytic fungi—alternative sources of cytotoxic compounds: a review. Front Pharmacol 2018;9:309.
[42] Wang L, Lu A-P, Yu Z-L, Wong RN, Bian Z-X, Kwok H-H, Yue PY-K, Zhou L-M, Chen H, Xu M. The melanogenesis-inhibitory effect and the percutaneous formulation of ginsenoside Rb1. PharmSciTech 2014;15(5):1252–62.
[43] Wang R-F, Li J, Hu H-J, Li J, Yang Y-B, Yang L, Wang Z-T. Chemical transformation and target preparation of saponins in stems and leaves of *Panax notoginseng*. J Ginseng Res 2018;42(3):270–6.
[44] Xie J, Wu Y-Y, Zhang T-Y, Zhang M-Y, Zhu W-W, Gullen EA, Wang Z-J, Cheng Y-C, Zhang Y-X. New and bioactive natural products from an endophyte of *Panax notoginseng*. Rsc Advances 2017;7(60):38100–9.
[45] Xiong Z-Q, Yang Y-Y, Zhao N, Wang YJBm. Diversity of endophytic fungi and screening of fungal paclitaxel producer from Anglojap yew, Taxus x media. BMC Microb 2013;13(1):71.
[46] Xu Y, Wang C, Liu H, Zhu G, Fu P, Wang L, Zhu W. Meroterpenoids and isocoumarinoids from a myrothecium fungus associated with apocynum venetum. Mar Drugs 2018;16(10):363.
[47] Yoon T-J, Lei TC, Yamaguchi Y, Batzer J, Wolber R, Hearing VJ. Reconstituted 3-dimensional human skin of various ethnic origins as an in vitro model for studies of pigmentation. Anal Biochem 2003;318(2):260–9.
[48] Yuan J, Jian-Nan B, Bing Y, Xu-Dong Z. Taxol-producing fungi: a new approach to industrial production of taxol. Chin J Biotechnol 2006;22(1):1–6.
[49] Zheng Y-K, Miao C-P, Chen H-H, Huang F-F, Xia Y-M, Chen Y-W, Zhao L-X. Endophytic fungi harbored in *Panax notoginseng*: diversity and potential as biological control agents against host plant pathogens of root-rot disease. J Ginseng Res 2017;41(3):353–60.
[50] Zhou H, Kepa JK, Siegel D, Miura S, Hiraki Y, Ross D. Benzene metabolite hydroquinone up-regulates chondromodulin-I and inhibits tube formation in human bone marrow endothelial cells. Mol Pharmacol 2009;76(3):579–87.
[51] Zhou X, Zhu H, Liu L, Lin J, Tang K. A review: recent advances and future prospects of taxol-producing endophytic fungi. Appl Microbiol Biotechnol 2010;86(6):1707–17.